

Dimension-6 Operator Analysis of the CLIC Sensitivity to New Physics

John Ellis ^{1,2}, Philipp Roloff ³, Verónica Sanz ⁴ and Tevong You ⁵

¹*Theoretical Particle Physics and Cosmology Group, Physics Department,
King's College London, London WC2R 2LS, UK*

²*Theoretical Physics Department, CERN, CH-1211 Geneva 23, Switzerland*

³*Experimental Physics Department, CERN, CH-1211 Geneva 23, Switzerland*

⁴*Department of Physics and Astronomy, University of Sussex, Brighton BN1 9QH, UK*

⁵*Cavendish Laboratory, University of Cambridge, J.J. Thomson Avenue,
Cambridge, CB3 0HE, UK;
DAMTP, University of Cambridge, Wilberforce Road, Cambridge, CB3 0WA, UK*

Abstract

We estimate the possible accuracies of measurements at the proposed CLIC e^+e^- collider of Higgs and W^+W^- production at centre-of-mass energies up to 3 TeV, incorporating also Higgsstrahlung projections at higher energies that had not been considered previously, and use them to explore the prospective CLIC sensitivities to decoupled new physics. We present the resulting constraints on the Wilson coefficients of dimension-6 operators in a model-independent approach based on the Standard Model effective field theory (SM EFT). The higher centre-of-mass energy of CLIC, compared to other projects such as the ILC and CEPC, gives it greater sensitivity to the coefficients of some of the operators we study. We find that CLIC Higgs measurements may be sensitive to new physics scales $\Lambda = \mathcal{O}(10)$ TeV for individual operators, reduced to $\mathcal{O}(1)$ TeV sensitivity for a global fit marginalising over the coefficients of all contributing operators. We give some examples of the corresponding prospective constraints on specific scenarios for physics beyond the SM, including stop quarks and the dilaton/radion.

1 Introduction

In view of the fact that, so far, the couplings of the known particles are consistent with those predicted in the Standard Model (SM), and in the absence of any evidence at the LHC or elsewhere of any particles beyond those in the SM, it is natural to assume that any new physics must involve massive particles that are decoupled at the energies explored so far [1]. Such models of new physics may be explored using the SM Effective Field Theory (SM EFT), which provides a model-independent parametrisation of the low-energy effects of such new physics via higher-dimensional operators constructed out of SM fields [2, 3]. In collider physics, operators of dimension 6 are typically the most important, since the dimension-5 Weinberg neutrino-mass operator [4] does not play a rôle ¹. Such operators may be generated at either tree or loop level, and in the latter case the matching to ultraviolet (UV) models is easily achieved by the universal one-loop effective action [7].

Data from the LHC, LEP and SLC have already been analysed using the SM EFT ² [8–21] in various choices of operator bases ³. In particular, three of us (JE, VS and TY) have published a global analysis of dimension-6 operators in the SM EFT [13], providing 95% CL ranges for their coefficients when marginalising over the possible coefficients of all contributing operators and when the operators are switched on individually, and similar global fits to dimension-6 operators can be found in, for example, Refs. [10, 12, 18]. The prospective sensitivities of future accelerators such as the HL-LHC, the ILC and FCC-ee have also been estimated [24–30].

We show in this paper that the Compact Linear Collider (CLIC) proposal for an e^+e^- collider with a centre-of-mass energy ≤ 3 TeV [31] has a unique advantage for probing the coefficients of dimension-6 operators in the SM EFT, and hence constraining scenarios for possible new physics beyond the SM. This is because the relative contributions of some dimension-6 operators to scattering amplitudes grow rapidly with the energy E , since interferences with SM amplitudes grow like E^2 relative to the latter, conferring a competitive advantage on a higher-energy collider that can attain measurement accuracies comparable with a lower-energy e^+e^- collider such as the ILC, FCC-ee or CEPC.

Previous studies of CLIC projections for Higgs physics focused on the WW fusion production mode that dominates Higgs production at higher energies [32]. Here we point out that associated HZ production at 1.4 and 3 TeV could be important for indirect new physics searches, despite the lower statistics. We had previously shown that the analogous Higgsstrahlung production mode at the LHC is particularly sensitive to certain dimension-6 operators whose contributions to the cross-section and kinematic distributions grow with energy [13] (See also Ref. [33]) ⁴. For the same reason, inclusion of associated HZ production has a dramatic effect on the SM EFT fit at CLIC.

The layout of this paper is as follows.

In Section 2 of this paper we recall relevant aspects of the SM EFT, highlighting the operators that contribute to processes measurable at CLIC at high energies, such as

¹For instances where dimension-8 operators may dominate, see for example Refs. [5, 6].

²See Ref. [22] and references therein for a review of the SM EFT.

³The **Rosetta** tool [23] may be used to translate between different operator bases used in the literature.

⁴The energy growth of dimension-6 operators has also been used to place constraints from Drell-Yan processes at hadron colliders [34].

Higgs production via both $e^+e^- \rightarrow HZ$ associated production and vector-boson fusion (VBF), and $e^+e^- \rightarrow W^+W^-$, which constrains SM EFT coefficients via triple-gauge couplings (TGCs). We also recall that there are some combinations of coefficients of dimension-6 operators that are particularly strongly constrained by electroweak precision tests (EWPTs).

In Section 3 of this paper we provide indicative estimates of the accuracy with which the cross sections for $e^+e^- \rightarrow HZ$ and $e^+e^- \rightarrow W^+W^-$ might be measurable at CLIC at centre-of-mass energies ranging from 350 GeV through 1.4 TeV to 3 TeV. We emphasise that these estimates are not yet based on detailed simulations, which are now being prepared by the CLICdp Collaboration. We also repurpose previous ILC studies to estimate how accurately Higgs observables could be measured at CLIC at 350 GeV.

In Section 4 we use these estimates to provide projections of the possible CLIC sensitivity to the coefficients of dimension-6 operators, treated both individually and marginalised in global fits. We provide numerical support for the claim made above that the higher-energy CLIC measurements could provide significantly improved sensitivity to some of these coefficients, precisely by virtue of the growth in their contributions to cross sections relative to calculations in the SM. We find that the dependence on certain operator coefficients may grow by a factor $\mathcal{O}(100)$ between 350 GeV and 3 TeV, leading to individual 95% CL sensitivities to new physics that may reach up ~ 10 TeV via certain operators whose contributions to cross-sections grow with energy.

Section 5 explores the applicability and utility of these CLIC estimates in the contexts of some specific scenarios for physics beyond the SM, namely stop squarks in the minimal supersymmetric extension of the SM (MSSM) and dilaton/radion models.

Finally, Section 6 summarises our conclusions, emphasising the importance of detailed simulations of CLIC data at high energies to justify and refine the estimates we make of the accuracies with which the $e^+e^- \rightarrow HZ$, $e^+e^- \rightarrow H\nu\bar{\nu}$ and $e^+e^- \rightarrow W^+W^-$ cross sections should be measurable at CLIC.

2 The Standard Model Effective Field Theory

In the Standard Model Effective Field Theory (SM EFT) it is assumed that all the known particles have exactly the same renormalisable couplings as predicted in the SM, but that these are supplemented by interactions characterised by higher-dimensional operators constructed out of SM fields. Thus, one considers all possible combinations of SM fields of a given dimensionality that are consistent with the SM $SU(3)_c \times SU(2)_L \times U(1)_Y$ gauge symmetries and Lorentz invariance. We focus here on the leading lepton-number-conserving dimension $d \geq 6$ operators, whose Wilson coefficients could be generated by decoupled new physics beyond the SM:

$$\mathcal{L}_{\text{SMEFT}} = \mathcal{L}_{\text{SM}} + \sum_i \frac{c_i}{\Lambda^2} \mathcal{O}_i. \quad (2.1)$$

The effects of operators with dimensions $d > 6$ are sub-dominant in such a decouplings scenario – with some exceptions [5] – justifying our focus on the dimension-6 terms in the SM EFT Lagrangian: For the purposes of our analysis, we express the dimension-6

operators \mathcal{O}_i in the basis of Ref. [12]. The dimensionful parameter Λ in (2.1) reflects the scale of the new decoupled physics, and the coefficients c_i are model-dependent. We assume CP conservation and a flavour-blind structure for the operators involving SM fermions, so that the operators relevant for the precision electroweak, Higgs and $e^+e^- \rightarrow W^+W^-$ observables that we include in our fits are those listed in Table 1.

EWPTs	Higgs Physics	TGCs
$\mathcal{O}_W = \frac{ig}{2} \left(H^\dagger \sigma^a \overleftrightarrow{D}^\mu H \right) D^\nu W_{\mu\nu}^a$		
$\mathcal{O}_B = \frac{ig'}{2} \left(H^\dagger \overleftrightarrow{D}^\mu H \right) \partial^\nu B_{\mu\nu}$		$\mathcal{O}_{3W} = g \frac{\epsilon_{abc}}{3!} W_\mu^{a\nu} W_{\nu\rho}^b W^{c\rho\mu}$
$\mathcal{O}_T = \frac{1}{2} \left(H^\dagger \overleftrightarrow{D}_\mu H \right)^2$	$\mathcal{O}_{HW} = ig(D^\mu H)^\dagger \sigma^a (D^\nu H) W_{\mu\nu}^a$	
$\mathcal{O}_{LL}^{(3)l} = (\bar{L}_L \sigma^a \gamma^\mu L_L) (\bar{L}_L \sigma^a \gamma_\mu L_L)$	$\mathcal{O}_{HB} = ig'(D^\mu H)^\dagger (D^\nu H) B_{\mu\nu}$	
$\mathcal{O}_R^e = (iH^\dagger \overleftrightarrow{D}_\mu H) (\bar{e}_R \gamma^\mu e_R)$	$\mathcal{O}_g = g_s^2 H ^2 G_{\mu\nu}^A G^{A\mu\nu}$	
$\mathcal{O}_R^u = (iH^\dagger \overleftrightarrow{D}_\mu H) (\bar{u}_R \gamma^\mu u_R)$	$\mathcal{O}_\gamma = g^2 H ^2 B_{\mu\nu} B^{\mu\nu}$	
$\mathcal{O}_R^d = (iH^\dagger \overleftrightarrow{D}_\mu H) (\bar{d}_R \gamma^\mu d_R)$	$\mathcal{O}_H = \frac{1}{2} (\partial^\mu H ^2)^2$	
$\mathcal{O}_L^{(3)q} = (iH^\dagger \sigma^a \overleftrightarrow{D}_\mu H) (\bar{Q}_L \sigma^a \gamma^\mu Q_L)$	$\mathcal{O}_f = y_f H ^2 \bar{F}_L H^{(c)} f_R + \text{h.c.}$	
$\mathcal{O}_L^q = (iH^\dagger \overleftrightarrow{D}_\mu H) (\bar{Q}_L \gamma^\mu Q_L)$	$\mathcal{O}_6 = \lambda H ^6$	

Table 1: List of pertinent CP-even dimension-6 operators in the basis [12] that we use. In each case we recall the categories of observables that provide the greatest sensitivities to the operator, possibly in combinations with other operators.

As noted in Table 1, electroweak precision tests (EWPTs), notably those in the leptonic sector of Z -pole observables, provide the greatest sensitivities to the following (combinations of) dimension-6 operators:

$$\mathcal{L}_{\text{dim-6}}^{\text{EWPT}} \supset \frac{1}{2} \frac{(\bar{c}_W + \bar{c}_B)}{m_W^2} (\mathcal{O}_W + \mathcal{O}_B) + \frac{\bar{c}_T}{v^2} \mathcal{O}_T + \frac{\bar{c}_{LL}^{(3)l}}{v^2} \mathcal{O}_{LL}^{(3)l} + \frac{\bar{c}_R^e}{v^2} \mathcal{O}_R^e. \quad (2.2)$$

In writing (2.2), we have introduced coefficients \bar{c}_i that differ from those in (2.1) by ratios of the squares of an electroweak scale M to the effective scale Λ of new physics:

$$\bar{c}_i = c_i \frac{M^2}{\Lambda^2}, \quad (2.3)$$

where $M \equiv m_W$ for the combination $\mathcal{O}_W + \mathcal{O}_B$, and $M \equiv v$ for the other operators.

As also noted in Table 1, the dimension-6 operators (and their linear combinations) relevant to the Higgs and triple-gauge coupling (TGC) measurements used in our fits are

$$\begin{aligned} \mathcal{L}_{\text{dim-6}}^{\text{Higgs+TGC}} \supset & \frac{1}{2} \frac{(\bar{c}_W - \bar{c}_B)}{m_W^2} (\mathcal{O}_W - \mathcal{O}_B) + \frac{\bar{c}_{HW}}{m_W^2} \mathcal{O}_{HW} + \frac{\bar{c}_{HB}}{m_W^2} \mathcal{O}_{HB} + \frac{\bar{c}_g}{m_W^2} \mathcal{O}_g + \frac{\bar{c}_\gamma}{m_W^2} \mathcal{O}_\gamma \\ & + \frac{\bar{c}_{3W}}{m_W^2} \mathcal{O}_{3W} + \frac{\bar{c}_H}{v^2} \mathcal{O}_H + \frac{\bar{c}_f}{v^2} \mathcal{O}_f. \end{aligned} \quad (2.4)$$

Since the EWPTs can constrain very strongly the linear combination $\bar{c}_W + \bar{c}_B$, we assume $\bar{c}_B = -\bar{c}_W$ when fitting Higgs and TGC measurements. When marginalising over the effects of all operators in our global fits this assumption holds less well for the TGCs [35], but is sufficient for our projections where we are mainly interested in a first estimate of the CLIC sensitivity to the scale of new physics ⁵.

Our fit constrains the coefficients at the respective centre-of-mass energy scales E at which they are measured: $c_i \equiv c_i(E)$, which are related to their values at the matching scale, $c_i(\Lambda)$, by renormalisation-group equations (RGEs) that we do not consider here [37]. Also, we neglect dimension-8 and higher-order operators in our analysis, as well as the four-fermion operators that do not interfere with the SM amplitudes [9] ⁶, whose effects on Z -pole measurements are of the same order in Λ (or M) as dimension-8 operators. It was pointed out in [15] that these operators and theory uncertainties that we omit could be relevant for $\Lambda \lesssim 3$ TeV. These effects and a consistent treatment of the SM EFT at one-loop level, including matching at one-loop [7], will become relevant for realistic fits as future precision data become available.

3 CLIC Measurements

The CLIC accelerator is foreseen to be built and operated in a staged approach with several centre-of-mass energy stages ranging from a few hundred GeV up to 3 TeV [31]. The CLIC physics potential for the measurement of a wide range of Higgs boson properties has been investigated in detail based on full detector simulations [32]. For our studies here, three energy stages at 350 GeV, 1.4 TeV and 3 TeV have been assumed.

CLIC at 350 GeV		CLIC at 1.4 TeV		CLIC at 3 TeV	
$\sigma_{H\nu_e\bar{\nu}_e}\text{BR}_{H\rightarrow b\bar{b}}$	1.9%	$\sigma_{H\nu_e\bar{\nu}_e}\text{BR}_{H\rightarrow b\bar{b}}$	0.4%	$\sigma_{H\nu_e\bar{\nu}_e}\text{BR}_{H\rightarrow b\bar{b}}$	0.3%
$\sigma_{HZ}\text{BR}_{H\rightarrow c\bar{c}}$	10.3%	$\sigma_{H\nu_e\bar{\nu}_e}\text{BR}_{H\rightarrow c\bar{c}}$	6.1%	$\sigma_{H\nu_e\bar{\nu}_e}\text{BR}_{H\rightarrow c\bar{c}}$	6.9%
$\sigma_{HZ}\text{BR}_{H\rightarrow gg}$	4.5%	$\sigma_{H\nu_e\bar{\nu}_e}\text{BR}_{H\rightarrow gg}$	5.0%	$\sigma_{H\nu_e\bar{\nu}_e}\text{BR}_{H\rightarrow gg}$	4.3%
$\sigma_{HZ}\text{BR}_{H\rightarrow W+W^-}$	5.1%	$\sigma_{H\nu_e\bar{\nu}_e}\text{BR}_{H\rightarrow W+W^-}$	1.0%	$\sigma_{H\nu_e\bar{\nu}_e}\text{BR}_{H\rightarrow W+W^-}$	0.7%
$\sigma_{HZ}\text{BR}_{H\rightarrow \tau\bar{\tau}}$	6.2%	$\sigma_{H\nu_e\bar{\nu}_e}\text{BR}_{H\rightarrow \tau\bar{\tau}}$	4.3%	$\sigma_{H\nu_e\bar{\nu}_e}\text{BR}_{H\rightarrow \tau\bar{\tau}}$	4.4%
$\sigma_{HZ}\text{BR}_{H\rightarrow b\bar{b}}$	0.84%	$\sigma_{H\nu_e\bar{\nu}_e}\text{BR}_{H\rightarrow \gamma\gamma}$	15.0%	$\sigma_{H\nu_e\bar{\nu}_e}\text{BR}_{H\rightarrow \gamma\gamma}$	10.0%
		$\sigma_{H\nu_e\bar{\nu}_e}\text{BR}_{H\rightarrow Z\gamma}$	42.0%	$\sigma_{H\nu_e\bar{\nu}_e}\text{BR}_{H\rightarrow Z\gamma}$	30.0%
		$\sigma_{H\nu_e\bar{\nu}_e}\text{BR}_{H\rightarrow ZZ}$	5.6%	$\sigma_{H\nu_e\bar{\nu}_e}\text{BR}_{H\rightarrow ZZ}$	3.9%

Table 2: Summary of projected statistical precisions for Higgs measurements from Ref. [32] that we use in our fit. Observables sourced elsewhere are discussed in the text.

For each of these three energy stages we use projected constraints on the Higgs measurements from Ref. [32], as summarised in Table 2. The Higgsstrahlung process dom-

⁵We note that the constraints on the individual coefficients of single operators switched on one at a time typically show a high level of sensitivity to new physics, but one typically expects several operators to be generated when integrating out heavy particles in any specific scenario for new physics [36].

⁶On the other hand, we do include $\bar{c}_{LL}^{(3)l}$ when analysing the EWPTs, which modifies the input parameter G_F .

inates most channels at 350 GeV, whereas vector-boson fusion (VBF) provides more statistics at 1.4 and 3 TeV, providing opportunities to identify and measure a wide range of Higgs decays. For the missing $H \rightarrow \gamma\gamma$, ZZ and $Z\gamma$ projections at 350 GeV we have treated them as in Ref. [24], assuming similar errors as for the ILC at 250 GeV. This is a good assumption if the errors in the branching ratios scale with the available number of Higgs bosons, which are similar for the ILC with 250 fb^{-1} at 250 GeV (assuming 80% polarization of the e^- beam and 30% polarization of the e^+ beam) to CLIC with 500 fb^{-1} at 350 GeV (with no polarization assumed).

Projections for some additional observables are needed for the analysis presented in this paper. Although VBF Higgs production dominates at 1.4 and 3 TeV, one of the main points of this work is to highlight the effect of including HZ associated production at high energies, and its importance for improving the sensitivity to certain dimension-6 operators. Also, the $e^+e^- \rightarrow W^+W^-$ process is important for constraining triple-gauge couplings that are important in global fits, as noted in Table 1. For these reasons, additional estimates have been made for the HZ and W^+W^- processes at generator level, including smearing and assuming the expected detector resolutions, where appropriate. These studies are summarised in the following. Confirmation of these results with full detector simulations and the study of potential systematic uncertainties are left for future analysis by the CLICdp Collaboration.

The cross sections and event samples were obtained using the WHIZARD 1.95 Monte Carlo program [38, 39]. The effects of initial-state radiation (ISR) and beamstrahlung were included in the generation. The expected precisions are normalised to an integrated luminosity of $500 \text{ fb}^{-1}/1.5 \text{ ab}^{-1}/2 \text{ ab}^{-1}$ at $\sqrt{s}=350 \text{ GeV}/1.4 \text{ TeV}/3 \text{ TeV}$.

3.1 Higgsstrahlung at High Energy

The process $e^+e^- \rightarrow HZ, Z \rightarrow q\bar{q}, H \rightarrow b\bar{b}$ was chosen to evaluate the expected uncertainty in the Higgsstrahlung cross section at 1.4 and 3 TeV, as it provides the largest event sample. All other processes resulting in four final-state quarks were considered as background. The four vectors of all final-state quarks were smeared assuming an energy resolution of: $\sigma(E)/E = 4\%$, which corresponds to the jet energy resolution of the CLIC detector models. The most probable Z and Higgs candidate in each event was selected by minimising:

$$\chi^2 = (m_{ij} - m_Z)^2/\sigma_Z^2 + (m_{kl} - m_H)^2/\sigma_H^2,$$

where m_{ij} and m_{kl} are the invariant masses of the quark pairs used to reconstruct the Z and Higgs boson candidates, respectively, and $\sigma_{Z,H}$ are the estimated invariant mass resolutions for hadronic decays of the Z and Higgs bosons. Events with a χ^2 minimum of less than 20 were considered further.

Two b-tags were required for each event. For this purpose, a b-tagging efficiency of 80%/10%/1% was assumed for beauty/charm/light quarks in the final state, as motivated by detailed simulations of realistic CLIC detector models. In order to exclude events with a large energy loss due to ISR or beamstrahlung, the HZ invariant mass was required to be larger than 1.3/2.8 TeV for a centre-of-mass energy of 1.4/3 TeV. After the selection

described above, the following uncertainties were obtained:

$$\frac{\Delta[\sigma(HZ) \cdot BR(H \rightarrow b\bar{b})]}{[\sigma(HZ) \cdot BR(H \rightarrow b\bar{b})]} = 3.3\% \text{ at } 1.4 \text{ TeV},$$

$$\frac{\Delta[\sigma(HZ) \cdot BR(H \rightarrow b\bar{b})]}{[\sigma(HZ) \cdot BR(H \rightarrow b\bar{b})]} = 6.8\% \text{ at } 3 \text{ TeV}.$$

3.2 Diboson production $e^+e^- \rightarrow W^+W^-$

The most promising final states to measure the cross section for the process $e^+e^- \rightarrow W^+W^-$ at CLIC are $q\bar{q}q\bar{q}$ and $q\bar{q}l^\pm\nu$, where l^\pm is an electron or muon. We assume that the background processes can be suppressed to a negligible level for a signal selection efficiency of 50% in both cases. Only events with a W^+W^- invariant mass above 330 GeV/1.3 TeV/2.8 TeV have been considered for $\sqrt{s} = 350 \text{ GeV}/1.4 \text{ TeV}/3 \text{ TeV}$, in order to exclude events in which ISR or beamstrahlung has a large impact. The following precisions are expected when combining both final states:

$$\frac{\Delta\sigma(W^+W^-)}{\sigma(W^+W^-)} = 0.1\% \text{ at } 350 \text{ GeV},$$

$$\frac{\Delta\sigma(W^+W^-)}{\sigma(W^+W^-)} = 0.2\% \text{ at } 1.4 \text{ TeV},$$

$$\frac{\Delta\sigma(W^+W^-)}{\sigma(W^+W^-)} = 0.3\% \text{ at } 3 \text{ TeV}.$$

4 Projections of CLIC Sensitivities

We now present the potential sensitivities to the coefficients of dimension-6 operators that could be provided by the projected measurements and their errors outlined in the previous section. There are no detailed studies of the sensitivity of CLIC to electroweak precision tests (EWPTs), so we omit such a projection here, referring instead to our previous work on the effects of dimension-6 operators on a leptonic subset of observables in future EWPTs [30].

The main operators affecting Higgs physics and triple-gauge couplings that are of interest for our analysis are \bar{c}_W , \bar{c}_{HW} , \bar{c}_{HB} , \bar{c}_{3W} , \bar{c}_γ and \bar{c}_g . We have calculated the linear dependences of the HZ Higgsstrahlung associated production cross-sections at 1.4 TeV and 3 TeV on these dimension-6 operator coefficients using `MadGraph5` [41], with the following numerical results:

$$\left. \frac{\Delta\sigma(HZ)}{\sigma(HZ)} \right|_{350 \text{ GeV}} = 16\bar{c}_{HW} + 4.7\bar{c}_{HB} + 35\bar{c}_W + 11\bar{c}_B - \bar{c}_H + 5.5\bar{c}_\gamma,$$

$$\left. \frac{\Delta\sigma(HZ)}{\sigma(HZ)} \right|_{1.4 \text{ TeV}} = 440\bar{c}_{HW} + 130\bar{c}_{HB} + 470\bar{c}_W + 121\bar{c}_B - \bar{c}_H + 7.3\bar{c}_\gamma,$$

$$\left. \frac{\Delta\sigma(HZ)}{\sigma(HZ)} \right|_{3 \text{ TeV}} = 2130\bar{c}_{HW} + 637\bar{c}_{HB} + 2150\bar{c}_W + 193\bar{c}_B - \bar{c}_H + 7.4\bar{c}_\gamma. \quad (4.1)$$

Similarly, in the cases of the $e^+e^- \rightarrow W^+W^-$ production cross-sections at 350 GeV, 1.4 TeV and 3 TeV, we obtain the following numerical results for the linear dependences on the dimension-6 operator coefficients:

$$\begin{aligned}
\left. \frac{\Delta\sigma(W^+W^-)}{\sigma(W^+W^-)} \right|_{350 \text{ GeV}} &= 0.63\bar{c}_{HW} + 0.31\bar{c}_{HB} + 4.6\bar{c}_W - 0.43\bar{c}_{3W}, \\
\left. \frac{\Delta\sigma(W^+W^-)}{\sigma(W^+W^-)} \right|_{1.4 \text{ TeV}} &= 3.8\bar{c}_{HW} + 2.2\bar{c}_{HB} + 7.9\bar{c}_W - 0.66\bar{c}_{3W}, \\
\left. \frac{\Delta\sigma(W^+W^-)}{\sigma(W^+W^-)} \right|_{3 \text{ TeV}} &= 13\bar{c}_{HW} + 7.8\bar{c}_{HB} + 17\bar{c}_W - 4.4\bar{c}_{3W}.
\end{aligned} \tag{4.2}$$

We see that the sensitivities to most of the operator coefficients increase substantially with the centre-of-mass energy, for both the Higgsstrahlung and W^+W^- cross-sections, confirming the expected competitive advantage of the high energies attainable with CLIC.

In particular, the Higgsstrahlung cross-section has a very strong dependence on energy for the dimension-6 operator coefficients \bar{c}_W , \bar{c}_{HW} and \bar{c}_{HB} , namely a factor $\mathcal{O}(100)$ between 350 GeV and 3 TeV. As an illustration, Fig. 1 displays the CLIC sensitivities to \bar{c}_{HW} for various centre-of-mass energies, also including estimates for 250 GeV and 420 GeV [42] that we do not include in our analysis. The horizontal dashed lines denote the corresponding projected experimental errors in the measurements, based on the estimates in Section 3 for 1.4 and 3 TeV and the recoil cross-section measurement for the lower energies, and the dots indicate the sensitivities to \bar{c}_{HW} that could be obtained by CLIC runs at these different energies, assuming that this is the only significant SM EFT effect. For comparison, the range of \bar{c}_{HW} values excluded by the individual limit obtained from Run 1 LHC data [13] is shaded in blue. We see that CLIC would improve marginally on this limit by running at 250 GeV, with substantial improvements possible with higher-energy runs.

Including all the various Higgs channels of Table 2, we have made global fits to estimate the sensitivities at the various CLIC centre-of-mass energies, using the dependences of the Higgs branching ratios on the dimension-6 operator coefficients provided by eHDECAY [43] in combination with the HZ production cross-section and the constraints on triple-gauge couplings from the W^+W^- production cross-section. In making our χ^2 fits, we assume Gaussian statistical errors and neglect theoretical uncertainties. The resulting 95% CL limits are plotted in Figs. 2, 3, and 4 for 350 GeV, 1.4 TeV and 3 TeV respectively.

The results from our 350 GeV fit shown in Fig. 2 include the individual limits obtained considering just one operator at a time colour-coded in green and the marginalised limits obtained including all operators in red. The lighter green bounds exclude the constraints coming from W^+W^- production. Comparing with the darker green bars that include W^+W^- production, we see that this process can help provide significantly stronger individual limits than can be obtained from Higgs physics alone. Moreover, we note that the \bar{c}_{3W} coefficient only affects triple-gauge couplings, so the inclusion of W^+W^- production is crucial in closing directions of limited sensitivity in marginalised fits. All Higgs observables and the W^+W^- cross section are included in the marginalised fit where all coefficients are allowed to vary simultaneously (including \bar{c}_f, \bar{c}_H , which we omit from these plots as the constraints on them are an order of magnitude worse).

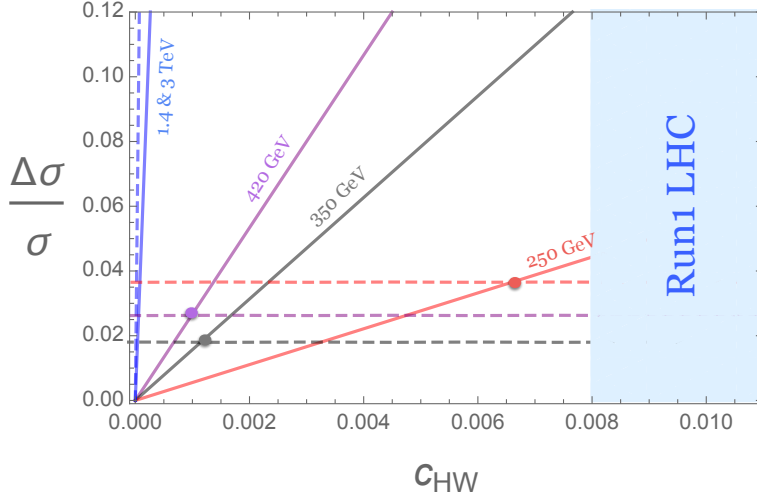


Figure 1: Illustration of the prospective CLIC sensitivities to the dimension-6 operator coefficient c_{HW} that could be obtained from measurements of the HZ Higgsstrahlung cross-section at different centre-of-mass energies. The diagonal solid lines represent the linear dependences shown in Eqs. (4.1, 4.2) and (4.3), and the horizontal dashed lines represent the measurement errors estimated in Section 3. The range excluded by data from Run 1 of the LHC is shaded blue.

The upper horizontal axis in Fig. 2 translates the limits on the barred coefficients to the corresponding scale of new physics Λ at which new physics with unit coupling would generate a coefficient of that size when being integrated out. We note that the actual scale would depend on the information encapsulated in the un-barred coefficients c_i , such as the coupling strength of the new physics and whether it is loop-induced or not. With this proviso, we see that the $\mathcal{O}(10^{-3})$ bounds in the 350 GeV fit translate to ~ 1 TeV sensitivities for the individual fits and ~ 800 GeV for the marginalised fit, with the notable exceptions of \bar{c}_γ and \bar{c}_g , which are many times more precise. We note in particular that \bar{c}_g is multiplied by 100 in Fig. 2, which is equivalent to Λ being multiplied by a factor of 10. As these two coefficients characterise loop-induced processes in the Standard Model, they are the most precise Higgs observables, and can place strong indirect limits on weakly-coupled loop-induced new physics such as stops in the MSSM.

The 1.4 TeV fits shown in Fig. 3 take into account, in addition to the Higgs channels of Table 2 and the W^+W^- cross-section of Section 3.2, also the HZ Higgsstrahlung production cross-section of Section 3.1. The individual limits shown in lightest green exclude both the HZ Higgsstrahlung and W^+W^- cross-section constraints, while those shown in olive green exclude the former but include the latter. The darkest green limits include both, as do the marginalised limits in red that now reach the ~ 1 TeV sensitivity for \bar{c}_W, \bar{c}_{HW} and \bar{c}_{HB} . This is largely driven by the inclusion of the Higgsstrahlung observable, which sets individual limits in the multi-TeV range for these operators. We

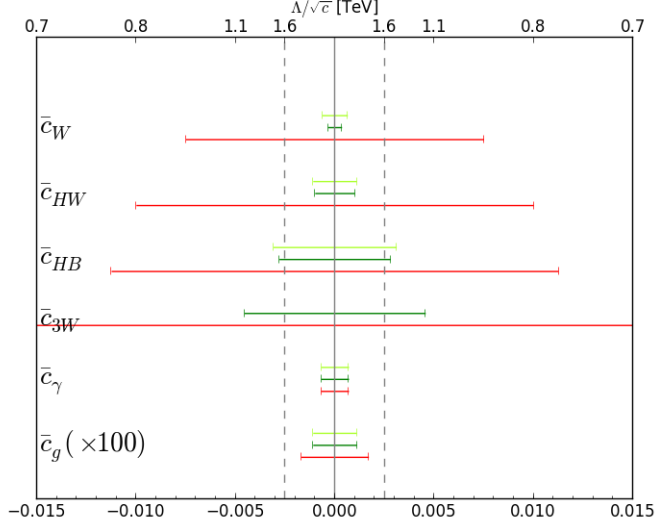


Figure 2: The prospective sensitivities of CLIC measurements at 350 GeV to individual operator coefficients (green) and in a fit marginalised over all contributing operators (red). The lighter green colour is for fits omitting the W^+W^- production cross-section.

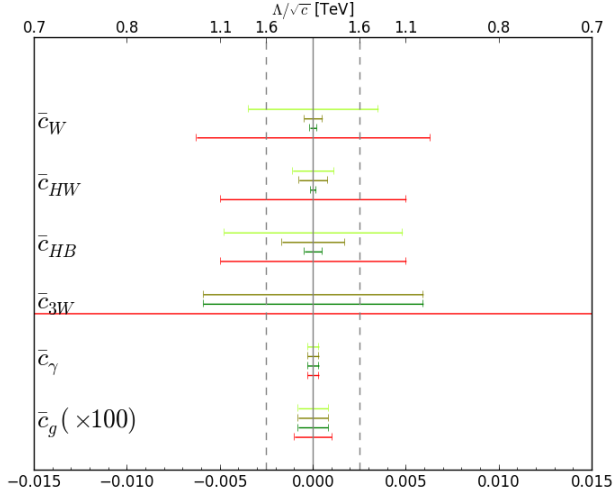


Figure 3: The prospective sensitivities of CLIC measurements at 1.4 TeV to individual operator coefficients (green) and in a fit marginalised over all contributing operators (red). The lightest green colour is for individual fits omitting both the HZ and W^+W^- production cross-sections, those in olive green exclude HZ but include W^+W^- , and the darkest green colour is for individual fits including both HZ and W^+W^- .

emphasise, however, that although the individual limits are beyond the centre-of-mass energy of 1.4 TeV, the marginalised limits allowing all relevant operators to vary simultaneously are generally < 1.4 TeV. A realistic model may have a scale in between, and it should be checked that one is still within the regime of validity of the SM EFT [6, 40].

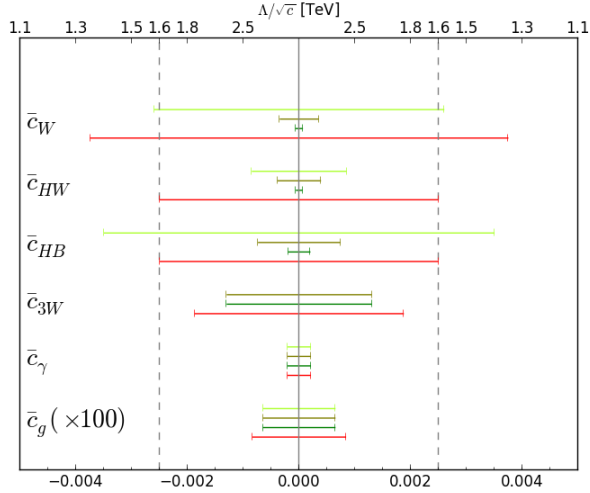


Figure 4: As for Fig. 3, but for CLIC measurements at 3 TeV.

Similar conclusions hold for the 3 TeV fits whose results are shown in Fig. 3, where the increases in sensitivity are even more marked, with individual limits on some operators reaching the 10 TeV level. This level of sensitivity becomes comparable to that at which future electroweak precision tests may constrain the orthogonal dimension-6 operator combination $\bar{c}_W + \bar{c}_B$. A complete fit will then have to be made that includes its effect simultaneously, including the RGE running neglected here, which mixes the coefficients at different energy scales [37].

The results for all three energies are summarised and compared side-by-side in the Fig. 5, where the different shades of green of the individual limit bars denote the effect of including (or not) the HZ Higgsstrahlung constraint. As seen in Eqns. 4.1, the increases with energy of the sensitivities of the operator coefficients \bar{c}_W , \bar{c}_B , \bar{c}_{HW} and \bar{c}_{HB} are the most rapid for this observable, and this is reflected in the increased heights of the lighter-coloured green bars seen in the left panel of Fig. 5. We conclude that measuring the associated production cross-section for $e^+e^- \rightarrow ZH$ increases significantly the CLIC sensitivities to these operator coefficients. On the other hand, the sensitivity to \bar{c}_{3W} is due exclusively to the W^+W^- cross-section observable, as seen in Eqns. 4.2. Finally, we note that the sensitivities to \bar{c}_γ and \bar{c}_g shown in the right panel of Fig. 5 increase relatively slowly with energy, as already seen in Eqns. 4.1.

Comparing with the analysis of ILC and FCC-ee sensitivities to individual SM EFT dimension-6 coefficients shown in Fig. 9 of [30], we see that CLIC data at 3.0 TeV would be significantly more sensitive to \bar{c}_{HW} and somewhat more sensitive to \bar{c}_{HB} , whereas the CLIC sensitivities at 1.4 TeV would be comparable to those attainable at ILC/FCC-ee. On the other hand, the CLIC sensitivity to \bar{c}_{3W} is weaker than ILC/FCC-ee. In the cases of \bar{c}_γ and \bar{c}_g , we see that CLIC could impose stronger constraints than the ILC, but weaker than FCC-ee.

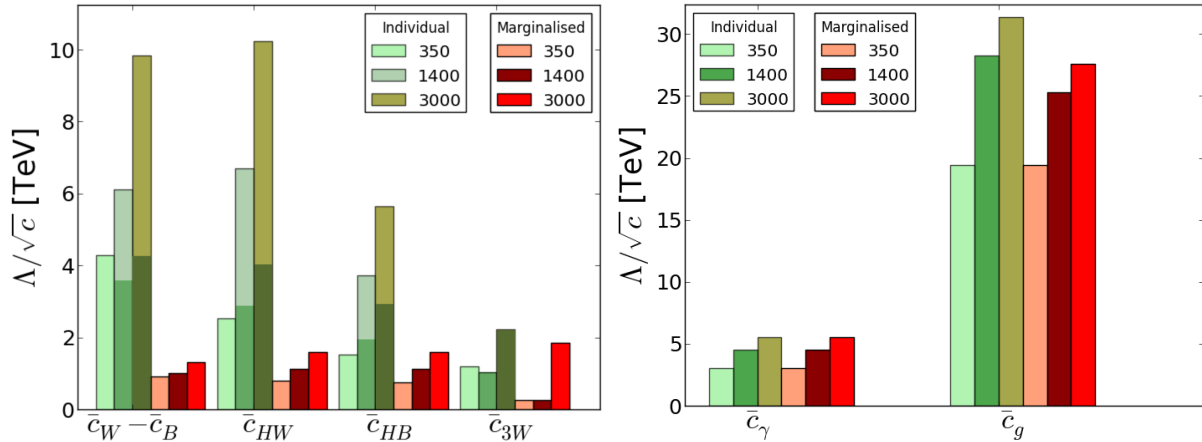


Figure 5: The estimated sensitivities of CLIC measurements at 350 GeV, 1.4 TeV and 3.0 TeV to the scales of various (combinations of) dimension-6 operator coefficients: $\bar{c}_W - \bar{c}_B$, \bar{c}_{HW} , \bar{c}_{HB} and \bar{c}_{3W} (left panel) and \bar{c}_γ and \bar{c}_g (right panel). The results of individual (marginalised) fits are shown as green (red) bars. The lighter (darker) green bars in the left panel include (omit) the prospective HZ Higgsstrahlung constraint.

5 The Reach of CLIC for Specific UV Scenarios

In order to contextualize the precision achieved by CLIC for the coefficients of the SM EFT operators, one may consider some specific models that could source the EFT coefficients. Accordingly we discuss in this Section two archetypical examples of UV completions of the EFT Lagrangian, specifically theories with more scalar particles beyond the Higgs boson, namely stops in the MSSM and a dilaton/radion model.

The phenomenology of these models has been widely studied, as well as their potential LHC signatures: see, e.g., [44] for a discussion of indirect constraints on stops with an explicit comparison of SM EFT and exact Feynman diagram calculations. In this connection, we note that direct searches for stops and other new scalars are necessarily model-dependent in nature, so that their reach is limited to specific assumptions and areas of parameter space, whereas indirect constraints are insensitive to assumptions about their production and decay modes. Indirect probes for new physics do not rely on the same set of assumptions as direct searches, and hence are a source of complementary information as well as a different way of finding new physics.

Virtual effects of stops in Higgs production via gluon fusion can be parametrized as an overall re-scaling of the rate, namely

$$\frac{\sigma(gg \rightarrow h)}{\sigma(gg \rightarrow h)_{SM}} = \kappa_g^2. \quad (5.1)$$

Loops of stops would induce modifications in the production rate of the Higgs as follows [45]:

$$\kappa_g = 1 + C_g(\alpha_s) \frac{F_g^{SUSY}}{F_g^{SM}} \quad (5.2)$$

where the SM loop contribution is proportional to $F_g^{SM} \simeq -2/1.41$, and $C_g(\alpha_s) = 1 + \frac{25\alpha_s}{6\pi}$. The function F_g encodes the effect of stops in loops, and is a function of the stop masses ($m_{\tilde{t}_{1,2}}$) and the mixing angle θ_t between the two chirality eigenstates:

$$F_g = -\frac{1}{3} \left[\frac{m_t^2}{m_{\tilde{t}_1}^2} + \frac{m_t^2}{m_{\tilde{t}_2}^2} - \frac{1}{4} \sin^2(2\theta_t) \frac{\Delta m^4}{m_{\tilde{t}_1}^2 m_{\tilde{t}_2}^2} \right]. \quad (5.3)$$

The best current bounds on κ_g come from combined the Run 1 analysis of Higgs properties by ATLAS and CMS [46], which reached a precision of about 20%, i.e., $\Delta\kappa_g = |\kappa_g - 1| \lesssim 0.2$ at 95% CL. Prospects for the High-Luminosity phase of the LHC (HL-LHC) are discussed in [47], and with 3000 fb⁻¹ an improvement by a factor of about 3 is expected, leading to $\Delta\kappa_g \simeq 6.7\%$.

One can translate the limit on κ_g in terms of the EFT coefficient \bar{c}_g that appears in the EFT framework, as follows:

$$\bar{c}_g = (\kappa_g - 1) \frac{F_g^{SM} m_W^2}{64\pi^2 v^2}. \quad (5.4)$$

In left panel of Fig. 6 we compare the current sensitivity to MSSM stops with the HL-LHC and CLIC prospects. We present the results in terms of the lightest stop eigenvalue $m_{\tilde{t}_1}$ and the mass separation from the heavier eigenstate $\Delta m^2 = m_{\tilde{t}_2}^2 - m_{\tilde{t}_1}^2$. We see that the current indirect limit on a light stop of around 200 GeV will improve by a factor of two with the full HL-LHC dataset. This reach would be surpassed by CLIC in any energy scenario. Specifically, in the case of CLIC at 350 GeV, we see that the sensitivity to $m_{\tilde{t}_1}$ is $\mathcal{O}(500)$ GeV, well beyond the direct production limit of 175 GeV, so the SM EFT is quite accurate in this case [44]. On the other hand, whereas the sensitivity with CLIC at 1.4 TeV is increased to $m_{\tilde{t}_1} \sim 600$ GeV, this is below the threshold at which the stop is integrated out and no better than the direct search sensitivity, while similarly the increased indirect sensitivity with CLIC at 3 TeV, $m_{\tilde{t}_1} \sim 700$ GeV is significantly less than the direct kinematic reach⁷. This is to be expected as the stops are mainly constrained by the \bar{c}_g operator coefficient that does not benefit from an energy growth in the cross-section at 1.4 and 3 TeV.

Another set of particularly interesting models is that with extended Higgs sectors, where massive scalar states could naturally evade discovery at the HL-LHC but lead to deviations in Higgs couplings that could be observed at CLIC. We focus here on the simplest such extension, namely a dilaton, or its dual, a radion scalar particle r . These new particles are dual to each other, and couple to the SM via the stress tensor T .

The radion/dilaton mass is linked to the mechanism of stabilization of the extra-dimension or the explicit breaking of dilatation symmetry. The result is very scenario-dependent, and it could be very light as well as around the scale of compactification (or spontaneous breaking) f , see e.g. [48, 49]. Integrating r out produces the effective Lagrangian one obtains the following effective Lagrangian [50]

$$\mathcal{L}_{eff} = -\frac{1}{f^2} \frac{1}{m_r^2} T^2 \quad (5.5)$$

⁷We note that our results are presented for a specific choice of the mixing angle $\theta_t = 0$, but the mass limits are roughly independent of the angle once other constraints such as $b \rightarrow s\gamma$ and m_W are taken into account [45].

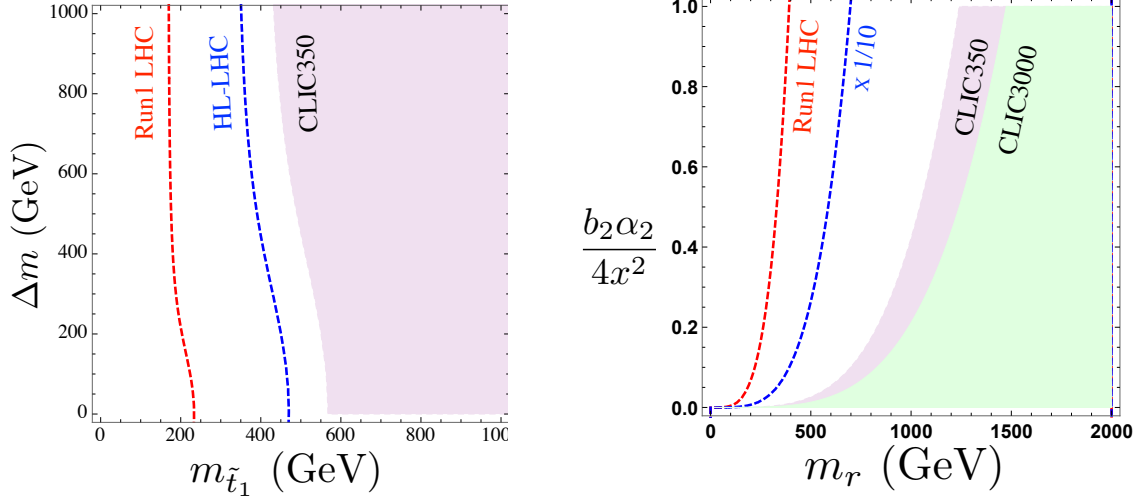


Figure 6: Mass reach for scenarios with new scalars. Boundaries correspond to 95% CL exclusions. (Left panel) Current and expected mass reach for interpretations of \bar{c}_g as limits on stop masses. (Right panel) Limits on the EFT coefficients interpreted in terms of the mass and coupling of the dilaton field, where the β -function coefficient b_2 and the parameter $x = f/m_r$ are introduced in the text.

where T is the trace of the stress-energy tensor. The relevant terms in the stress tensor for the Higgs and gauge bosons are

$$T \subset -2 |D_\mu \Phi|^2 + 4 V(\Phi^\dagger \Phi) - \frac{b_i \alpha_i}{8\pi} F_{\mu\nu}^i F^{i\mu\nu} , \quad (5.6)$$

where $V = -m_h^2 |\Phi|^2 + \lambda |\Phi|^4$ and the b_i are the β -function coefficients, which lead to anomalous violations of scale invariance. The values of the b_i depend on the degree of compositeness of fermions in the SM and possible new physics contributions. For example, in conformal field theories (CFTs) one typically obtains, $b_i^{CFT} = 8\pi^2 / (g_i^2 \log(\mu_{IR}/\Lambda_{UV}))$ [49], in which case

$$b_2 \alpha_2 \simeq 2\pi \log(\mu_{IR}/\Lambda_{UV}) . \quad (5.7)$$

One can easily read off the following coefficients of dimension-6 operators:

$$\begin{aligned} \bar{c}_{HW} = -\bar{c}_W &= -\frac{b_2 \alpha_2}{4} \frac{m_h^2 v^2}{f^2 m_r^2} , \\ \bar{c}_{HB} = -\bar{c}_B &= -\frac{b_1 \alpha_1}{4} \frac{m_h^2 v^2}{f^2 m_r^2} . \end{aligned} \quad (5.8)$$

One could also consider a more general situation with a non-universal dilaton/radion coupling. This would lead to a prefactor in the coefficients of the effective operators, dependent on the degree of overlap of the wavefunctions in the bulk (radion) or participation on the composite dynamics of the species (dilaton), but we do not enter into details here.

The dominant dilaton/radion production mechanism at CLIC would be in association with a Z boson, $e^+e^- \rightarrow Z \rightarrow Zr$. In the case of CLIC at 350 GeV, the production cross-section scales as $\sim 1 \text{ pb} (1 \text{ TeV}/f)^2$ for $m_r \lesssim 200 \text{ GeV}$, and at 3.0 TeV CLIC would produce 1-TeV radions with a cross-section $0.5 \text{ pb} (1 \text{ TeV}/f)^2$. In models where the composite dynamics is related to the origin of electroweak symmetry breaking, one finds that the radion/dilaton decays predominantly to massive particles whenever kinematically allowed, with ratios $2 : 1 : 1$ to the final states W^+W^- , ZZ and hh respectively [51]. Therefore the signatures at the LHC are dominated by diboson decays, which are most distinctive in the high-mass region (above a TeV).

We show in the right panel of Fig. 6 indirect limits on the radion parameter space via the effect on the SM EFT with the constraints $\bar{c}_{HW} = -\bar{c}_W$ and $\bar{c}_W + \bar{c}_B \simeq 0$. We also compare with the limits from the Run-I fit [13] and an optimistic ballpark estimate of an improvement of a factor ten for \bar{c}_{HW} in the high-luminosity LHC runs. We see that CLIC can extend the indirect reach for the radion mass into the TeV scale, greatly exceeding the direct reach of the LHC. However, we note that for CLIC at 3 TeV the exclusion contour extends into a region where the EFT expansion breaks down, though there could still be indirect probes of the radion via the behaviour of the Higgs.

As far as direct searches are concerned, we note that a non-universal dilaton/radion could decay predominantly to an invisible final state or one that is particularly difficult to detect. At 3 TeV, the cross section for e^+e^- to neutrinos and a Z boson is 2 pb, much larger than the cross section expected in the dilaton/radion model considered here. So, if the radion/dilaton decays into invisible (undetected) final states, further kinematic selections would be needed to distinguish new phenomena from the neutrino background. This example illustrates the complementarity between indirect and direct probes, as they are based on different assumptions about the couplings to SM particles and dominant branching ratios.

The gain in sensitivity for CLIC at 1.4 and 3 TeV comes from the energy dependence of certain operators that can place tight constraints on their Wilson coefficients. However, if the mass scale of the UV physics being integrated out lies below the kinematic threshold then the parameter space of such models is outside the regime of EFT validity. On the other hand, in some strongly-coupled models the UV mass scale may lie significantly beyond this validity threshold [6, 33]. This may occur if there is a strong coupling whose degeneracy with the UV mass scale can maintain a fixed value for the Wilson coefficient's contribution to the cross-section. For example, Ref. [33] discusses a model of composite fermions whose effects in Higgsstrahlung can be generated by $\bar{c}_W - \bar{c}_B$ via such a strong coupling. Such a scenario would be beyond the direct reach of CLIC but may still be probed indirectly in the higher-energy runs with an SM EFT analysis.

6 Summary and Conclusions

We have emphasized in this paper the potential importance of measurements of $e^+e^- \rightarrow HZ$, $H\nu\bar{\nu}$ and W^+W^- in high-energy CLIC running for indirectly probing possible new physics beyond the SM by constraining the coefficients of dimension-6 operators in the SM EFT. We have stressed, and shown numerically, that the increased relative importance

of interferences between SM and dimension-6 EFT amplitudes at high energies provides opportunities in the processes $e^+e^- \rightarrow HZ$ and W^+W^- , in particular.

These processes have not yet been simulated in detail by the CLICdp Collaboration [31, 32], so we have presented estimates of the prospective precision with which their cross-sections could be measured in CLIC running at 1.4 and 3 TeV. We have then incorporated these estimates in fits of the relevant SM EFT coefficients, showing that such measurements are orders of magnitude more sensitive than low-energy measurements. In some cases, the sensitivity to new physics in individual dimension-6 operator coefficients may reach the level of 10 TeV, greater than that attainable with the ILC or FCC-ee [30].

We matched the coefficients on to specific UV models and analysed the implications for the indirect sensitivity to new particles in these scenarios. We find that CLIC at 350 GeV may outperform the indirect constraints from LHC and HL-LHC on stops and radions/dilatons. The 1.4 and 3 TeV runs, on the other hand, are uniquely sensitive to operators whose contributions to the Higgsstrahlung process grows with energy. They may be used to constrain specific strongly-coupled models of composite fermions that are inaccessible to direct searches.

Our results motivate more detailed studies including additional benchmark analyses based on full CLIC detector simulations at high energies, with the aim of verifying and refining our estimates of the accuracies with which the cross-sections for $e^+e^- \rightarrow HZ$ and W^+W^- could be measured at CLIC. It has long been clear that the higher centre-of-mass energies attainable with CLIC offer significant advantages in direct searches for heavy particles that appear in scenarios for physics beyond the SM. The results of our paper indicate that the same should be true for indirect searches for such new physics.

Acknowledgements

The research of JE has been supported partly by the Science Technology and Facilities Council (STFC) under grant ST/L000326/1, and the research of VS has been supported partly by the STFC under grant ST/J000477/1. TY is supported by a Research Fellowship from Gonville and Caius College, Cambridge.

References

- [1] T. Appelquist and J. Carazzone, Phys. Rev. D **11** (1975) 285
- [2] W. Buchmuller and D. Wyler, Nucl. Phys. B **268** (1986) 621.
- [3] B. Grzadkowski, M. Iskrzynski, M. Misiak and J. Rosiek, JHEP **1010**, 085 (2010) [arXiv:1008.4884 [hep-ph]].
- [4] S. Weinberg, Phys. Rev. Lett. **43** (1979) 1566.
- [5] A. Azatov, R. Contino, C. S. Machado and F. Riva, arXiv:1607.05236 [hep-ph].
- [6] R. Contino, A. Falkowski, F. Goertz, C. Grojean and F. Riva, JHEP **1607** (2016) 144 doi:10.1007/JHEP07(2016)144 [arXiv:1604.06444 [hep-ph]].
- [7] B. Henning, X. Lu and H. Murayama, JHEP **1601** (2016) 023 doi:10.1007/JHEP01(2016)023 [arXiv:1412.1837 [hep-ph]]; A. Drozd, J. Ellis, J. Quéville and T. You, JHEP **1506** (2015) 028 [arXiv:1504.02409 [hep-ph]]; S. A. R. Ellis, J. Quéville, T. You and Z. HZang, Phys. Lett. B **762** (2016) 166 doi:10.1016/j.physletb.2016.09.016 [arXiv:1604.02445 [hep-ph]] and in preparation.
- [8] B. Grinstein and M. B. Wise, Phys.Lett. B **265** (1991) 326334. K. Hagiwara, S. Ishihara, R. Szalapski and D. Zeppenfeld, Phys. Rev. D **48**, 2182 (1993). K. Hagiwara, R. Szalapski and D. Zeppenfeld, Phys. Lett. B **318**, 155 (1993) [hep-ph/9308347].
- [9] Z. Han and W. Skiba, Phys. Rev. D **71** (2005) 075009 [hep-ph/0412166].
- [10] T. Corbett, O. J. P. Eboli, J. Gonzalez-Fraile and M. C. Gonzalez-Garcia, arXiv:1211.4580 [hep-ph]; B. Dumont, S. Fichet and G. von Gersdorff, JHEP **1307**, 065 (2013) [arXiv:1304.3369 [hep-ph]].
- [11] M. Ciuchini, E. Franco, S. Mishima and L. Silvestrini, JHEP **1308** (2013) 106 [arXiv:1306.4644 [hep-ph]]. M. Ciuchini, E. Franco, S. Mishima, M. Pierini, L. Reina and L. Silvestrini, Nucl. Part. Phys. Proc. **273-275** (2016) 2219 doi:10.1016/j.nuclphysbps.2015.09.361 [arXiv:1410.6940 [hep-ph]].
- [12] A. Pomarol and F. Riva, JHEP **1401** (2014) 151 [arXiv:1308.2803 [hep-ph]].
- [13] J. Ellis, V. Sanz and T. You, JHEP **1407** (2014) 036 [arXiv:1404.3667 [hep-ph]]. J. Ellis, V. Sanz and T. You, JHEP **1503** (2015) 157 [arXiv:1410.7703 [hep-ph]].
- [14] A. Falkowski and F. Riva, JHEP **1502** (2015) 039 [arXiv:1411.0669 [hep-ph]].
- [15] L. Berthier and M. Trott, JHEP **1505** (2015) 024 [arXiv:1502.02570 [hep-ph]]; JHEP **1602** (2016) 069 doi:10.1007/JHEP02(2016)069 [arXiv:1508.05060 [hep-ph]].
- [16] A. Efrati, A. Falkowski and Y. Soreq, JHEP **1507** (2015) 018 [arXiv:1503.07872 [hep-ph]].

- [17] A. Falkowski, *Pramana* **87** (2016), 39 doi:10.1007/s12043-016-1251-5 [arXiv:1505.00046 [hep-ph]].
- [18] T. Corbett, O. J. P. Eboli, D. Goncalves, J. Gonzalez-Fraile, T. Plehn and M. Rauch, *JHEP* **1508** (2015) 156 [arXiv:1505.05516 [hep-ph]].
- [19] A. Buckley, C. Englert, J. Ferrando, D. J. Miller, L. Moore, M. Russell and C. D. White, *Phys. Rev. D* **92** (2015), 091501 doi:10.1103/PhysRevD.92.091501 [arXiv:1506.08845 [hep-ph]].
- [20] A. Falkowski, M. Gonzalez-Alonso, A. Greljo and D. Marzocca, *Phys. Rev. Lett.* **116** (2016), 011801 doi:10.1103/PhysRevLett.116.011801 [arXiv:1508.00581 [hep-ph]].
- [21] J. Brehmer, A. Freitas, D. Lopez-Val and T. Plehn, *Phys. Rev. D* **93** (2016) no.7, 075014 doi:10.1103/PhysRevD.93.075014 [arXiv:1510.03443 [hep-ph]].
- [22] D. de Florian *et al.* [LHC Higgs Cross Section Working Group], arXiv:1610.07922 [hep-ph].
- [23] A. Falkowski, B. Fuks, K. Mawatari, K. Mimasu, F. Riva and V. Sanz, *Eur. Phys. J. C* **75** (2015), 583 doi:10.1140/epjc/s10052-015-3806-x [arXiv:1508.05895 [hep-ph]].
- [24] D. M. Asner *et al.*, *ILC Higgs White Paper*, arXiv:1310.0763 [hep-ph].
- [25] A. Freitas, K. Hagiwara, S. Heinemeyer, P. Langacker, K. Moenig, M. Tanabashi and G. W. Wilson, *Exploring Quantum Physics at the ILC*, arXiv:1307.3962 [hep-ph].
- [26] T. Han, Z. Liu, Z. Qian and J. Sayre, *Phys. Rev. D* **91** (2015) 113007 [arXiv:1504.01399 [hep-ph]]. G. Moortgat-Pick *et al.*, *Eur. Phys. J. C* **75** (2015) 8, 371 [arXiv:1504.01726 [hep-ph]]. K. Fujii *et al.*, *Physics Case for the International Linear Collider*, arXiv:1506.05992 [hep-ex].
- [27] T. Barklow, J. Brau, K. Fujii, J. Gao, J. List, N. Walker and K. Yokoya, *ILC Operating Scenarios*, arXiv:1506.07830 [hep-ex].
- [28] M. Bicer *et al.* [TLEP Design Study Working Group Collaboration], *JHEP* **1401** (2014) 164 [arXiv:1308.6176 [hep-ex]].
- [29] M. Baak *et al.*, *Working Group Report: Precision Study of Electroweak Interactions*, arXiv:1310.6708 [hep-ph]; J. Fan, M. Reece and L. T. Wang, *JHEP* **1509** (2015) 196 doi:10.1007/JHEP09(2015)196 [arXiv:1411.1054 [hep-ph]]; J. Fan, M. Reece and L. T. Wang, *JHEP* **1508** (2015) 152 [arXiv:1412.3107 [hep-ph]]; A. Thamm, R. Torre and A. Wulzer, *JHEP* **1507** (2015) 100 [arXiv:1502.01701 [hep-ph]];
- [30] J. Ellis and T. You, *JHEP* **1603** (2016) 089 doi:10.1007/JHEP03(2016)089 [arXiv:1510.04561 [hep-ph]].

- [31] M. J. Boland *et al.* [CLIC and CLICdp Collaborations], *Updated baseline for a staged Compact Linear Collider*, doi:10.5170/CERN-2016-004 arXiv:1608.07537 [physics.acc-ph].
- [32] H. Abramowicz *et al.*, *Higgs Physics at the CLIC Electron-Positron Linear Collider*, arXiv:1608.07538 [hep-ex].
- [33] A. Biekter, A. Knochel, M. Krämer, D. Liu and F. Riva, Phys. Rev. D **91** (2015) 055029 doi:10.1103/PhysRevD.91.055029 [arXiv:1406.7320 [hep-ph]].
- [34] M. Farina, G. Panico, D. Pappadopulo, J. T. Ruderman, R. Torre and A. Wulzer, arXiv:1609.08157 [hep-ph].
- [35] Z. Zhang, Phys. Rev. Lett. **118** (2017) no.1, 011803 doi:10.1103/PhysRevLett.118.011803 [arXiv:1610.01618 [hep-ph]].
- [36] Y. Jiang and M. Trott, arXiv:1612.02040 [hep-ph].
- [37] C. Grojean, E. E. Jenkins, A. V. Manohar and M. Trott, JHEP **1304** (2013) 016 [arXiv:1301.2588 [hep-ph]]; J. Elias-Miro, J. R. Espinosa, E. Masso and A. Pomarol, JHEP **1308** (2013) 033 [arXiv:1302.5661 [hep-ph]]; J. Elias-Miro, J. R. Espinosa, E. Masso and A. Pomarol, JHEP **1311** (2013) 066 [arXiv:1308.1879 [hep-ph]]; E. E. Jenkins, A. V. Manohar and M. Trott, JHEP **1310** (2013) 087 [arXiv:1308.2627 [hep-ph]]; E. E. Jenkins, A. V. Manohar and M. Trott, JHEP **1401** (2014) 035 [arXiv:1310.4838 [hep-ph]]; R. Alonso, E. E. Jenkins, A. V. Manohar and M. Trott, JHEP **1404** (2014) 159 doi:10.1007/JHEP04(2014)159 [arXiv:1312.2014 [hep-ph]]; J. Elias-Miro, C. Grojean, R. S. Gupta and D. Marzocca, JHEP **1405** (2014) 019 doi:10.1007/JHEP05(2014)019 [arXiv:1312.2928 [hep-ph]]; R. Alonso, H. M. Chang, E. E. Jenkins, A. V. Manohar and B. Shotwell, Phys. Lett. B **734** (2014) 302 [arXiv:1405.0486 [hep-ph]].
- [38] W. Kilian, T. Ohl and J. Reuter, Eur. Phys. J. C **71** (2011) 1742 doi:10.1140/epjc/s10052-011-1742-y [arXiv:0708.4233 [hep-ph]].
- [39] M. Moretti, T. Ohl and J. Reuter, *O'Mega: An Optimizing matrix element generator*, hep-ph/0102195.
- [40] A. Falkowski, M. Gonzalez-Alonso, A. Greljo, D. Marzocca and M. Son, arXiv:1609.06312 [hep-ph].
- [41] J. Alwall, M. Herquet, F. Maltoni, O. Mattelaer and T. Stelzer, JHEP **1106**, 128 (2011) [arXiv:1106.0522 [hep-ph]].
- [42] M. Thomson, Eur. Phys. J. C **76** (2016), 72 doi:10.1140/epjc/s10052-016-3911-5 [arXiv:1509.02853 [hep-ex]].
- [43] R. Contino, M. Ghezzi, C. Grojean, M. Muhlleitner and M. Spira, Comput. Phys. Commun. **185** (2014) 3412 doi:10.1016/j.cpc.2014.06.028 [arXiv:1403.3381 [hep-ph]].

- [44] A. Drozd, J. Ellis, J. Quevillon and T. You, JHEP **1506** (2015) 028
doi:10.1007/JHEP06(2015)028 [arXiv:1504.02409 [hep-ph]].
- [45] J. R. Espinosa, C. Grojean, V. Sanz and M. Trott, JHEP **1212** (2012) 077
doi:10.1007/JHEP12(2012)077 [arXiv:1207.7355 [hep-ph]].
- [46] G. Aad *et al.* [ATLAS and CMS Collaborations], JHEP **1608**, 045 (2016)
doi:10.1007/JHEP08(2016)045 [arXiv:1606.02266 [hep-ex]].
- [47] ATLAS Collaboration, *Projections for measurements of Higgs boson signal strengths and coupling parameters with the ATLAS detector at a HL-LHC*,
<https://cds.cern.ch/record/1956710/files/ATL-PHYS-PUB-2014-016.pdf>.
- [48] W. D. Goldberger and M. B. Wise, Phys. Rev. Lett. **83**, 4922 (1999)
[hep-ph/9907447].
- [49] W. D. Goldberger, B. Grinstein and W. Skiba, Phys. Rev. Lett. **100** (2008) 111802
[arXiv:0708.1463 [hep-ph]]. W. D. Goldberger and M. B. Wise, Phys. Lett. B **475**,
275 (2000) [hep-ph/9911457]. C. Csaki, M. L. Graesser and G. D. Kribs, Phys.
Rev. D **63** (2001) 065002 [hep-th/0008151].
- [50] M. Gorbahn, J. M. No and V. Sanz, JHEP **1510** (2015) 036
doi:10.1007/JHEP10(2015)036 [arXiv:1502.07352 [hep-ph]].
- [51] M. Gouzevitch, A. Oliveira, J. Rojo, R. Rosenfeld, G. P. Salam and V. Sanz, JHEP
1307, 148 (2013) doi:10.1007/JHEP07(2013)148 [arXiv:1303.6636 [hep-ph]].